Intermixing and buried interfacial structure in strained Ge/Si(105) facets

L. Fazi,[1] C. Hogan,[2,1,3] L. Persichetti,[1,4] C. Goletti,[1] M. Palummo,[1,3] A. Sgarlata,[1] and A. Balzarotti[1]
[1]*Dipartimento di Fisica, Università di Roma "Tor Vergata", Via della Ricerca Scientifica, 1-00133 Roma, Italy*
[2]*Istituto di Struttura della Materia, Consiglio Nazionale delle Ricerche (CNR-ISM), via Fosso del Cavaliere 100, 00133 Roma, Italy*
[3]*European Theoretical Spectroscopy Facility (ETSF)*
[4]*CHOSE (Centre for Hybrid and Organic Solar Energy), Università di Roma "Tor Vergata"*
(Received 25 June 2013; revised manuscript received 25 October 2013; published 26 November 2013)

The strained {105} facet, fundamental in the heteroepitaxial growth of Ge/Si(100), is investigated through a combination of scanning tunneling microscopy, reflectance anisotropy spectroscopy, and density functional theory simulations. Besides providing a strong independent confirmation of the proposed structural model, optical measurements give insight into Si/Ge intermixing, reveal hidden signatures of the buried interface, and give access to a complementary viewpoint of the epitaxial growth with respect to standard top-layer probing. Strained subsurface atoms are found to strongly determine the electronic and optical properties of the whole reconstruction. Moreover, we demonstrate how their unique spectral fingerprint is a sensitive probe of the local chemical bonding environment and allows the stoichiometry of atomic bonds to be monitored within and beneath the surface layer.

DOI: 10.1103/PhysRevB.88.195312 PACS number(s): 68.37.Ef, 73.20.−r, 78.68.+m

The continuous drive towards semiconductor technology miniaturization has lead to increased interest in the spontaneous formation of coherent islands during Stranski-Krastanow growth of strained epitaxial layers.[1,2] In this context, Ge on Si(001) is considered a prototypical model system for studying the fundamental mechanisms of strain relaxation in lattice-mismatched semiconductors,[3,4] as well as for modeling the electronic and optical properties of three-dimensional (3D) heterostructures.[5] Extensive experimental and theoretical investigations have shown that the evolutionary pathway observed for Ge/Si(001) epitaxy is mainly dictated by the stability of {105} facets of Ge and SiGe pyramidal islands and *huts*.[6–9] Similar facets have also been identified in nanoripples on the Ge/Si(1 1 10) surface[10,11] and on ultrathin Ge nanowires grown on Si(001).[12]

The peculiar geometry of the rebonded-step (RS) reconstruction of the {105} facets has been established,[9,13,14] and its key role in promoting misfit strain relief and determining the elastic properties of Ge islands has been demonstrated.[15–17] In contrast, its electronic structure and optical properties remain largely unknown. This is likely due to the narrow size of island facets (a few square nanometers), which hinders the use of most experimental probes. However, on vicinal Si surfaces close to the (105) plane, the misfit strain of Ge epitaxy stabilizes a *singular* crystal face which appears to be completely RS reconstructed.[13,18] Following deposition of a few monolayers (MLs) of Ge on Si(105), scanning tunneling microscopy (STM) measurements indicate that the RS reconstruction, appearing as zigzag rows orthogonal to the [010] direction, forms on wide, single-domain, atomically flat terraces [Fig. 1(a)]. This is in sharp contrast to the narrow RS facets observed on Ge islands grown on flat Si(001) [Fig. 1(b)].

In this work we demonstrate how reflectance anisotropy spectroscopy (RAS) combined with density functional theory (DFT) simulations provides insight into Si/Ge intermixing and buried interface structure in Si/Ge systems, in particular, by probing the stoichiometry *below* the topmost layers of the Ge/Si(105) surface. This application of RAS is complementary to its long-exploited use in real-time monitoring of top-layer epitaxial growth.[19,20] We show how strained subsurface bonds of the RS reconstruction, which are hidden from probe microscopy, strongly determine the electronic and optical properties of the whole reconstruction, defining true surface states inside the projected bulk band gap. From their unique spectral fingerprints, being extremely sensitive to the local chemical bonding environment, the standard RAS technique yields direct insight into the composition of the Ge/Si system, distinguishing between pure and mixed regions, believed to occur at least at the base of the Ge/Si quantum dot,[21] and elucidating the unusual stability of the RS-reconstructed {105} facets.[22] Besides revealing hidden signatures of the buried interface, our study provides a strong independent confirmation of the proposed surface reconstruction model.[9,13–15]

The geometry of the RS reconstruction is shown in Fig. 2(a) for a 4-ML coverage[23] of Ge. It comprises pairs of six-atom "horseshoe" moieties that can be understood as groupings of three dimers: two (a–b and e–f) being considerably stretched, tilted upwards, and having a filled dangling bond each; the third (c–d) being more relaxed, weakly tilted, and having two dangling bonds. Although dimers are the principle reconstruction element on Si(001), the horseshoe block is only stable in a strained environment, with the larger elastic constant of Ge allowing the necessary flexibility in bond lengths and torsion angles. As such, it is one of the largest single reconstruction motifs observed, along with tetramer-interstitial (TI) or pentamer units found on Si(331)-(12 × 1),[24] Ge(113), and Ge/Si(113),[25] and Si or Ge(110)-(16 × 2) surfaces.[26] Unlike these adatom-stabilized reconstruction units, however, which yield distinctive pentamer patterns in the STM topography, previously reported images for the RS-reconstructed {105} facet[9,13] do not reflect the local atomic geometries in any obvious way, with both filled and empty state images simply appearing as two bright spots per cell. As previously discussed,[13] this stems from a large redistribution of charge among the constituent dimers, suggesting that STM is hardly intuitive for characterizing the RS reconstruction; such charge transfer can instead be probed

 ©2013 American Physical Society

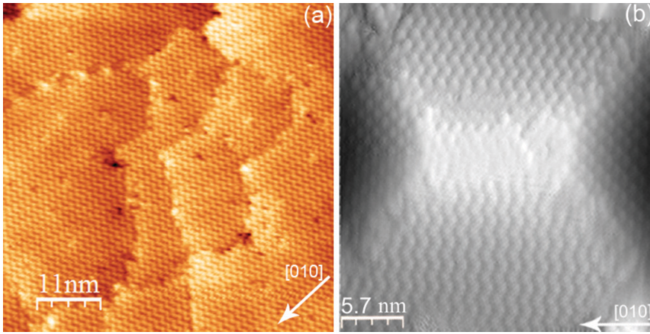

FIG. 1. (Color online) STM images of (a) the RS-reconstructed Ge/Si(105) surface at a coverage of ∼4 ML of Ge, and (b) a Ge/Si(001) pyramid showing RS-reconstructed {105} facets.

using a Kelvin-probe method with atomic force microscopy.[14] In the following we will demonstrate that RAS offers an alternative, powerful diagnostic approach for investigating the system.

We begin by analyzing the overall Ge/Si(105) surface quality using STM, since a high-quality preparation is a stringent requirement for any surface optical measurement. Experiments were carried out in ultrahigh vacuum ($p < 4 \times 10^{-11}$ mbar) on vicinal Si(001) wafers miscut by 11.5° towards the [100] direction. The RS reconstruction was prepared through physical vapor deposition of Ge at room temperature followed by annealing to 870 K. The deposition rate was 0.3 ML/min. Room-temperature STM images are shown in Fig. 2(b), where they are compared with DFT-LDA (density functional theory in the local-density approximation) simulations obtained within the Tersoff-Hamann approach at constant current.[27,28] For the latter, we used thick (22 Å) RS-reconstructed slabs with lateral lattice constants fixed to that of bulk Si (5.40 Å) in order to reproduce the effect of

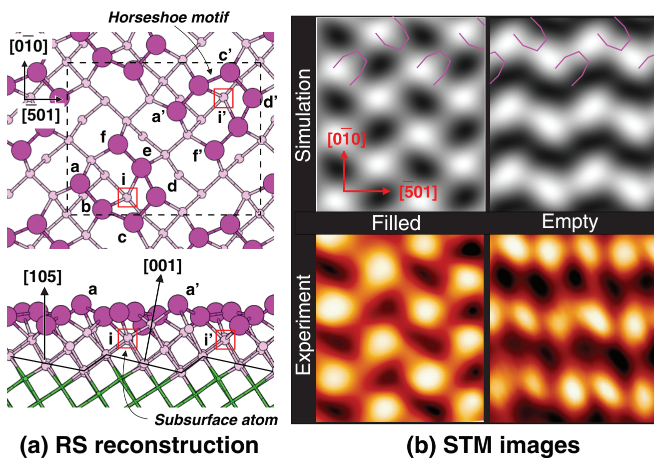

FIG. 2. (Color online) (a) Schematic structure (top and side views) of the Ge/Si(105) rebonded-step surface reconstruction for a 4-ML Ge coverage. Pink circles are Ge; subsurface Si layers are shown below (in green). Dashed lines show the surface unit cell. (b) Experimental and simulated STM images (28 × 33) Å^2 for filled ($V = -1.5$ V; $I = 1.5$ nA) and empty ($V = +1.0$ V; $I = 0.7$ nA) states at constant current.

strain in the Ge layers. The simulated images for a 4-ML Ge coverage, shown in Fig. 2(b), appear in good agreement with previous works[9,13] and with our measured profiles for both positive and negative biases.

The chainlike pattern observed along [$\bar{5}$01] in the empty state STM images nonetheless hints at a strong electronic *anisotropy*, even though the local and global geometric pattern appears, at first glance, quite symmetric. This, coupled with the presence of wide and equally oriented terraces as visible in Fig. 1(a), prompts the use of RAS: being an optical technique, it is sensitive to buried interfaces and symmetry lowering through surface strain, and can probe growth processes *in situ*. RAS experiments were carried out using a compact homemade apparatus in the version with two polarizers.[29] The RAS signal ($\Delta R/R$) is obtained by the normalized difference of the reflectance R for light linearly polarized in two orthogonal directions of the sample surface plane, and is defined as $\Delta R/R = (R_{[\bar{5}01]} - R_{[0\bar{1}0]})/\langle R \rangle$, where $R_{[\bar{5}01]}$ and $R_{[0\bar{1}0]}$ are the square moduli of the Fresnel coefficients for light polarized along directions [$\bar{5}$01] and [0$\bar{1}$0], that are parallel and perpendicular to the zigzag rows of atoms visible in Fig. 1(a).

The measured RAS signals for clean and Ge-covered Si(105) are reported in Fig. 3(a). To eliminate spurious contributions from the optical setup, the residual anisotropy (optical background) of the oxidized surface ($\Delta R/R^{\mathrm{oxid}}$) has been subtracted from each experimental curve. As previously reported,[13,18,30] clean Si(105) is atomically rough and does not show a stable reconstruction or long-range order. The RAS response at high photon energies is actually a sensitive indicator of this roughness. The almost linear decrease of the optical anisotropy observed in the 3–5 eV range can be modeled within the classical effective medium theory of Bruggeman[31] assuming a surface roughness in the range 5–8 Å, a value which is consistent with the roughness of clean Si(105) at the scale size probed by RAS. Instead, the spectrum in the surface sensitive range (below 3.4 eV) exhibits only a weak oscillatory line shape.

After 4 ML of Ge deposition, the RAS spectrum [Fig. 3(a)] shows strong oscillations near the bulk critical points at 3.3–3.7 eV. It is well known that at bulk critical points RAS detects characteristic anisotropy features related to strain, band bending, sample doping, temperature, and bulk symmetry properties.[32] As our spectra have been reported as $\Delta R/R - \Delta R/R^{\mathrm{oxid}}$, and different strain and (presumably) band bendings occur after annealing of the surface, the resulting difference is difficult to interpret. More importantly, completely new spectral features appear below 3.2 eV: a peak P at 2.1 eV, and a shoulder S around 2.5 eV that is most likely the signature of an additional component in the spectrum. Oxidation experiments support the surface origin of P: following exposure to 1500 L of high-purity molecular oxygen, the peak completely disappears. This exposure value is typical for surface states (an initial sticking coefficient S_0 in the 10^{-3} range can be estimated from optical data).[33,34] Moreover, STM data demonstrate that the disappearance of the RS reconstruction and the progressive attenuation of the peak are totally entangled. We note that maximum RAS intensity is obtained for light polarized along the [$\bar{5}$01] direction, i.e., along the long axis of the RS cell. This confirms that the

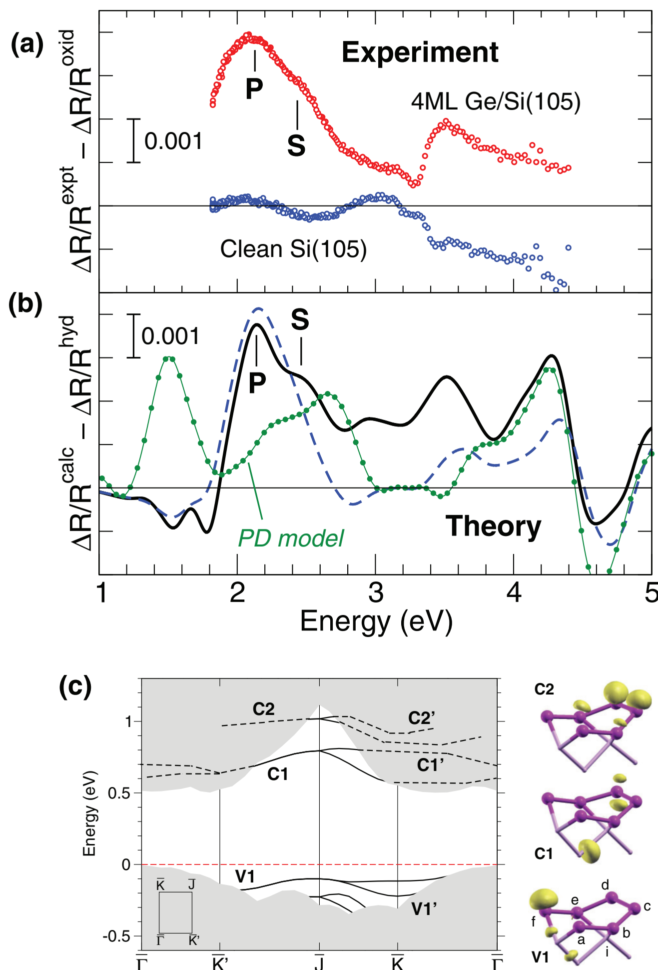

FIG. 3. (Color online) (a) Measured RAS spectra for the clean Si(105) surface (lower curve, blue), and after absorption of 4 ML of Ge and annealing at 870 K (upper curve, red). The residual optical anisotropy (measured at the fully oxidized surface) has been subtracted in each case. (b) Computed RAS spectra at 4 ML Ge of the RS reconstruction model with (dashed line) and without (solid line) subtraction of the optical background (hydrogenated surface), compared with the signal for the PD model (dotted line). A Lorentzian broadening of 0.15 eV is used. (c) DFT-LDA band structure of the 4-ML coverage slab, superimposed on the projected bulk band structure of silicon, plotted within a quarter of the surface Brillouin zone (see inset: $\bar{\Gamma}$–$\bar{K}$ corresponds to the $[0\bar{1}0]$ direction). Band splitting derives from the presence of two horseshoe units per cell. Isosurfaces of $|\psi|^2$ near the $\bar{J}$ point for selected surface states are shown with respect to the atoms of the horseshoe structure [Fig. 2(a)].

optical signal is closely correlated to the spatial orientation of the surface electronic states.

In parallel, RAS spectra were simulated by means of *ab initio* calculations of the (anisotropic) surface dielectric tensor and bulk dielectric function.[35] The surface response function was extracted from that of the RS-reconstructed, H-terminated slab by appropriate means of a real-space cutoff technique.[36] Calculations were performed at the independent particle (IP) level, and a scissors operator of +0.4 eV was applied to account for the well-known underestimation of the band gap within DFT-LDA.[37,38] As a first approximation, we assume that the Ge overlayer forms a sharp interface with the Si substrate [see Fig. 2(a)].

Computed spectra at 4 ML of Ge are shown in Fig. 3(b), both as raw data and with a suitable background signal subtracted. (We chose the hydrogen-passivated surface, as the structure is better defined.) The results are in very good agreement with the experimental curve, regarding both the line shape and amplitude. (Differences above 3.5 eV are an artefact of the background subtraction.) For comparison, we also show the computed signal from the paired dimer (PD) model of Mo *et al.*,[39] previously discounted on the basis of several studies.[9,13,14] Although its RAS signal exhibits several peaks of the correct sign [consistent with the (105) step orientation], their position and intensity are very different from those of the RS model. These results therefore constitute an independent confirmation of the RS reconstruction model.

Analysis of the calculated spectra (i.e., through analysis of the slab dielectric tensor) reveals some interesting, unexpected features. Firstly, both P and S are found to arise from transitions between occupied states lying about 1 eV below the valence band maximum (namely, extended surface resonances or surface-perturbed bulk states) and empty surface-localized states nearer to the gap. As delocalized, bulklike states are relatively insensitive to surface perturbations, RAS here yields an almost *direct* probe of the unoccupied surface bands, clearly identified as such in the electronic band structure [Fig. 3(c)]. Secondly, the principle feature P is due to transitions involving the lowest unoccupied state C1 (or C1′), that we note is not associated directly with the top layer atoms. Instead, it is mostly localized 4 Å below the top atomic layer, at the strained backbond of the *subsurface* atom i. Although atom i appears to be regularly coordinated with the surrounding atoms, it is in fact sixfold coordinated, being weakly bonded also to the atoms c,d of the third dimer (distance 2.73 Å; other bonds are 2.4–2.58 Å). This character recalls the sixfold coordinated interstitial atom that supports the tetramer of adatoms in the TI model. Later we will show that C1 and i, being physically located below the surface, allow us to obtain insight into subsurface growth processes. The shoulder S instead involves transitions to the top dimer antibonding states C2/C2′. We note that a Ge-dimer-related peak at 2.5 eV has been previously reported on the Ge(100)-(2 × 1) surface,[40] consistent with our interpretation of the structure.

Up to now we have assumed that the Ge/Si(105) reconstruction is composed of a uniform Ge layer forming a sharp interface with the Si substrate. It is interesting to investigate whether this assumption is valid, as some intermixing between Si and Ge is expected at 870 K: besides entropic effects, activation energies for Si/Ge exchange as low as 0.6 eV have been reported.[41] Nonetheless, it is difficult to distinguish between Si and Ge atoms in topmost layers using tunneling microscopy or spectroscopy alone.[42] RAS, in contrast, offers a heightened sensitivity. In Fig. 4 we show the computed RAS signal for the RS reconstruction model at a 4-ML Ge coverage, but assuming different (inter)mixing random configurations. We consider three cases: (i) a sharp interface as before; (ii) a "gradual" interface whereby Ge atoms fill the topmost layers (including atom i), being otherwise smoothly redistributed to deeper layers; and (iii) a "diffuse" interface in which each monolayer possesses a 50% Ge/Si intermixing.

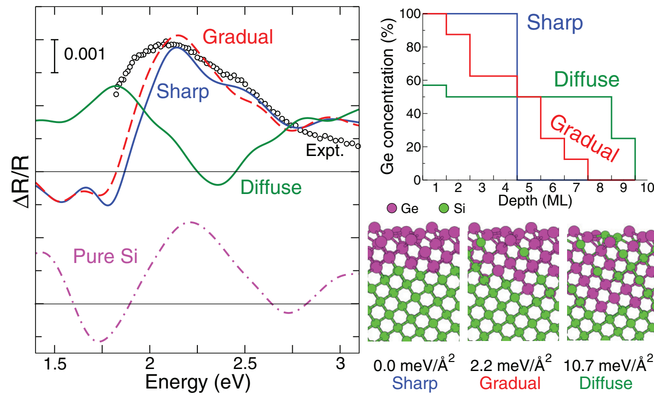

FIG. 4. (Color online) Left: Computed RAS signals at a 4-ML coverage for different interface compositions, compared with experiment (dots) and a pure silicon RS-reconstructed slab (below). Right: Corresponding depth profile of Ge, and side views of the structures used in the simulations.

The corresponding Ge concentration is plotted alongside as a function of depth [in terms of (001) monolayers], and formation energies of the three structures, relative to that of the sharp interface, are reported. We also plot the computed spectrum for a pure silicon RS-reconstructed slab.

Although this study is by no means exhaustive, a number of conclusions may be drawn. First, the RAS signal for the "diffuse" interface differs strongly from all other spectra—including the experimental data—implying that the topmost layers are predominantly composed of Ge. Second, the "sharp" and "gradual" curves are very similar, indicating that intermixing of Si and Ge may well be present below the topmost surface layers. These observations are consistent with the computed formation energies: while the "sharp" and "gradual" interfaces are very close in energy, suggesting that intermixing may be present at the interface of the true Ge/Si(105) system, higher energy "diffuse"-like patterns are relatively unfavored.[43] Such disorder may partially explain why the measured RAS peak appears broader than the computed one. Third, we note that the computed signal for a pure silicon configuration (not experimentally observed) has a strong positive feature near 2.2 eV, similar to that of the "sharp" Ge/Si signal at 4 ML. This suggests that reconstructions uniformly composed of Si–Si or Ge–Ge bonds possess a similar optical anisotropy.

These results demonstrate that, even in an isovalent Si/Ge system, RAS is sensitive to the local stoichiometry—in other words, Si–Ge bonds produce a different optical response with respect to Ge–Ge or Si–Si bonds that can be detected with the technique. Such sensitivity is highest, however, for the surface layers, and is less evident in deeper layers. In the specific case of Ge/Si(105), this indicates that the top 1–2 ML are (almost fully) composed of Ge, while Si/Ge intermixing may be present below the surface, i.e., at the interface, for higher coverages. In the following, we demonstrate how RAS can furthermore be used to monitor the changing local stoichiometry at the Ge/Si interface as the Ge coverage θ increases.

Figure 5(a) shows STM surface topographies for post-annealed surfaces at $\theta = 1, 2,$ and 4 ML of Ge; the corresponding evolution of the RAS signal in the surface-sensitive regime is reported in Fig. 5(b). An appropriate background signal (in this case, the unreconstructed Ge-covered surface) has been subtracted in each case. Except for a lower concentration of defects and somewhat wider terraces, STM shows that the morphological changes are minimal on the topmost layer. Within the same coverage range, nonetheless, we observe a significant evolution of RAS spectra during the growth. Notably, both P and S signals undergo nontrivial energetic shifts up until saturation is reached. This indicates changing structural and electronic properties with coverage, as distinct from simple domain enlargement.[44] Our DFT-IP calculations of the RAS for increasing values of θ qualitatively reproduce these trends, as shown in Fig. 5(c). Differences may be due to some intermixing (as mentioned before), the larger defect presence at lower coverages in the experiment, and uncertainty in the measured coverage. The overall agreement with experiment nonetheless

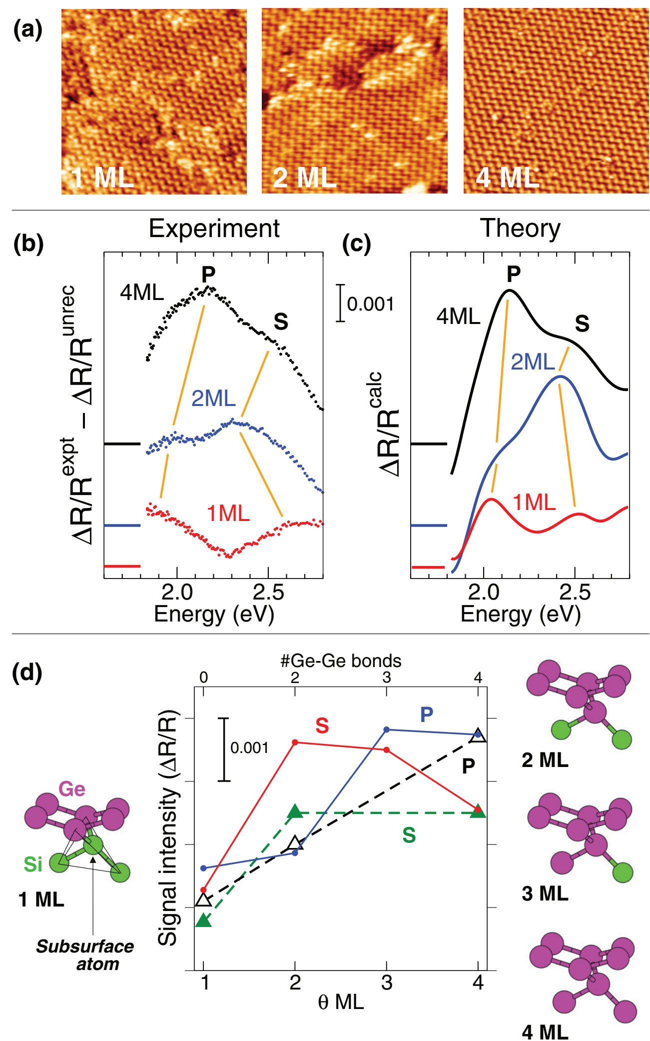

FIG. 5. (Color online) (a) STM images (50 × 50 Å^2) of the (105) surface for increasing coverage θ of Ge. (b) Measured RAS spectra near the main peak position for different θ. The signal from the unreconstructed surface has been subtracted in each case. Lines are a guide to the eye. Baselines are indicated on the left. (c) Calculated spectra. (d) Intensities of the P and S features as a function of θ (experiment: dashed lines; theory: solid lines). The corresponding number of nearest-neighbor Ge-Ge bonds in the subsurface tetrahedron and changes in stoichiometry are indicated.

supports our assumption that growth proceeds through a downward, layer-by-layer mechanism, whereby almost full Ge layers form below the RS-reconstructed layers which altogether "float" on the silicon substrate.[41] This trend thereby acts to stabilize the RS-reconstructed domains on a wider scale.

Theory can therefore be used to link the observed spectral changes with structural changes occurring during growth. We stress that, notwithstanding some relaxation, the simulated reconstruction geometry remains the same throughout; structural modifications thus consist of compositional (Si/Ge substitution) changes in the buried interfacial layers. By analyzing the optically active states involved in the main spectral features, we follow the trends in peak position and intensity with coverage, and thus probe the changing local chemical environment of the surface states. Trends in measured and computed intensities for both P and S features are plotted in Fig. 5(d) as a function of θ. As a quantitative measure, we also indicate the corresponding number of Ge–Ge bonds formed by atom i with its nearest neighbors (at $\theta = 1$ ML, i is silicon).

We note that (1) the relative strengths of P and S switch for $\theta \geqslant 3$ ML as the environment of i becomes more uniform (Ge-like); (2) the intensity of S sharply jumps at $\theta = 2$ ML, reflecting the abrupt change in C2 as the c–d dimer "backbonds" to atom i change character from Si–Ge to Ge–Ge. The initial importance of S can thus be traced back to its origin in states of the top-layer dimers, which are likely the first reconstruction elements to form. As the full horseshoe unit and its backbonds stabilize, P begins to dominate the spectrum. Therefore, RAS directly reflects the changing chemistry of both surface and subsurface atomic bonds, and allows us to identify the stoichiometry of single bonds below the surface. It is noteworthy that the access to the compositional changes of the buried interface is obtained here with a compact laboratory apparatus and without the need of synchrotron radiation, as in the case of x-ray diffraction.[45]

As a final remark, we note that the horseshoe structure and its associated states behave as a single coherent unit, and not, for instance, like a protective cap of the interfacial layers below. This is reflected both in the experimental oxidation measurements, which report uniform quenching with O coverage, and also in the theoretical simulations of the hydrogenated surface. In the latter, H not only saturates the surface dimer bonds, but concomitantly removes the subsurface strain around atom i, quenching *all* surface states uniformly. Thus, while RAS is sensitive to local changes in bond composition during growth, passivation instead is manifested as a uniform change across the observed spectrum.

In conclusion, by exploiting Si(105) vicinals as a model system, we unveiled the electronic properties and optical fingerprints of the RS reconstruction observed on the strained Ge/Si(105) surface and on the {105} facets of Ge/Si(001) quantum dots. Combined experimental and theoretical data showed a close connection between the spectral features and the distinctive structural motifs of the RS reconstruction. Being sensitive to the local chemical bonding environment, RAS is shown to directly probe the changing stoichiometry of the buried interface during adlayer growth. This allows us to distinguish between disordered Si-Ge and pure Ge-Ge sequences in surface and subsurface atomic bonds, suggesting an approach, with respect to standard methods, for probing top-layer epitaxial growth of semiconductors.

C.H. and M.P. acknowledge high-performance supercomputing resources and support from CINECA through the ISCRA initiative. The theoretical part of this work has been carried out as ETSF User Project No. 467. L.P. acknowledges support from the Regione Lazio project GESTO. We thank M. Fanfoni for useful discussions and acknowledge valuable technical contributions from M. Iannilli and G. Vitali for interfacing the RAS apparatus to the STM chamber.

[1] J. Stangl, V. Holý, and G. Bauer, Rev. Mod. Phys. **76**, 725 (2004).
[2] J. N. Aqua, I. Berbezier, L. Favre, T. Frisch, and A. Ronda, Phys. Rep. **522**, 59 (2013).
[3] B. Voigtländer, Surf. Sci. Rep. **43**, 127 (2001).
[4] F. Ratto and F. Rosei, Mater. Sci. Eng., R **70**, 243 (2010).
[5] K. Brunner, Rep. Prog. Phys. **65**, 27 (2002).
[6] P. Sutter and M. G. Lagally, Phys. Rev. Lett. **84**, 4637 (2000).
[7] J. Tersoff, B. J. Spencer, A. Rastelli, and H. von Kanel, Phys. Rev. Lett. **89**, 196104 (2002).
[8] G. H. Lu and F. Liu, Phys. Rev. Lett. **94**, 176103 (2005).
[9] P. Raiteri, D. B. Migas, L. Miglio, A. Rastelli, and H. von Kanel, Phys. Rev. Lett. **88**, 256103 (2002).
[10] P. D. Szkutnik, A. Sgarlata, A. Balzarotti, N. Motta, A. Ronda, and I. Berbezier, Phys. Rev. B **75**, 033305 (2007).
[11] G. Chen, B. Sanduijav, D. Matei, G. Springholz, D. Scopece, M. J. Beck, F. Montalenti, and L. Miglio, Phys. Rev. Lett. **108**, 055503 (2012).
[12] J. J. Zhang, G. Katsaros, F. Montalenti, D. Scopece, R. O. Rezaev, C. Mickel, B. Rellinghaus, L. Miglio, S. De Franceschi, A. Rastelli, and O. G. Schmidt, Phys. Rev. Lett. **109**, 085502 (2012).
[13] Y. Fujikawa, K. Akiyama, T. Nagao, T. Sakurai, M. G. Lagally, T. Hashimoto, Y. Morikawa, and K. Terakura, Phys. Rev. Lett. **88**, 176101 (2002).
[14] T. Eguchi, Y. Fujikawa, K. Akiyama, T. An, M. Ono, T. Hashimoto, Y. Morikawa, K. Terakura, T. Sakurai, M. G. Lagally, and Y. Hasegawa, Phys. Rev. Lett. **93**, 266102 (2004).
[15] D. B. Migas, S. Cereda, F. Montalenti, and L. Miglio, Surf. Sci. **556**, 121 (2004).
[16] G. H. Lu, M. Cuma, and F. Liu, Phys. Rev. B **72**, 125415 (2005).
[17] D. Scopece, F. Montalenti, and M. J. Beck, Phys. Rev. B **85**, 085312 (2012).
[18] L. Persichetti, A. Sgarlata, G. Mattoni, M. Fanfoni, and A. Balzarotti, Phys. Rev. B **85**, 195314 (2012).
[19] J. P. Harbison, D. E. Aspnes, A. A. Studna, L. T. Florez, and M. K. Kelly, Appl. Phys. Lett. **52**, 2046 (1988).
[20] A. R. Turner, M. E. Pemble, J. M. Fernández, B. A. Joyce, J. Zhang, and A. G. Taylor, Phys. Rev. Lett. **74**, 3213 (1995).
[21] A. Malachias, T. U. Schülli, G. Medeiros-Ribeiro, L. G. Cançado, M. Stoffel, O. G. Schmidt, T. H. Metzger, and R. Magalhães-Paniago, Phys. Rev. B **72**, 165315 (2005).

[22]L. Persichetti, A. Sgarlata, M. Fanfoni, and A. Balzarotti, Phys. Rev. Lett. **104**, 036104 (2010).

[23]For convenience, we report the thickness of Ge epilayers in units of (001) MLs, where 1 ML (001) $\simeq$ 2.55 ML (105).

[24]C. Battaglia, K. Gaál-Nagy, C. Monney, C. Didiot, E. F. Schwier, M. G. Garnier, G. Onida, and P. Aebi, Phys. Rev. Lett. **102**, 066102 (2009).

[25]D. Scopece and M. J. Beck, Phys. Rev. B **87**, 155310 (2013).

[26]T. An, M. Yoshimura, I. Ono, and K. Ueda, Phys. Rev. B **61**, 3006 (2000).

[27]P. Giannozzi *et al.*, J. Phys.: Condens. Matter **21**, 395502 (2009); and http://www.quantum-espresso.org.

[28]Plane waves (30 Ry cutoff) and norm-conserving pseudopotentials (including core corrections for Ge) were used along with $(2 \times 2 \times 1)$ k-point meshes. Back surfaces, passivated with H, were kept fixed during relaxation.

[29]A. Salvati and P. Chiaradia, Appl. Opt. **39**, 5820 (2000); C. Goletti, G. Bussetti, P. Chiaradia, A. Sassella, and A. Borghesi, Org. Electron. **5**, 73 (2004).

[30]M. Tomitori, K. Watanabe, M. Kobayashi, F. Iwawaki, and O. Nishikawa, Surf. Sci. **301**, 214 (1994).

[31]D. J. Bergman, Phys. Rep. **43**, 377 (1978).

[32]L. F. Lastras-Martínez, M. Chavira-Rodríguez, R. E. Balderas-Navarro, J. M. Flores-Camacho, and A. Lastras-Martínez, Phys. Rev. B **70**, 035306 (2004); L. F. Lastras-Martínez, J. M. Flores-Camacho, R. E. Balderas-Navarro, M. Chavira-Rodríguez, A. Lastras-Martínez, and M. Cardona, *ibid.* **75**, 235315 (2007).

[33]C. Goletti, P. Chiaradia, L. Moretti, W. Yian, G. Chiarotti, and S. Selci, Surf. Sci. **356**, 68 (1996).

[34]G. Chiarotti, P. Chiaradia, E. Faiella, and C. Goletti, Surf. Sci. **453**, 112 (2000).

[35]F. Bechstedt, *Principles of Surface Physics* (Springer-Verlag, Berlin, 2003).

[36]C. Hogan, R. Del Sole, and G. Onida, Phys. Rev. B **68**, 035405 (2003).

[37]Denser (8×4) k-point meshes were used for the optical spectra. The scissors shift (0.4 eV) is computed from the difference between the experimental E2 critical point energy (4.25 eV) and the computed value (3.85 eV), hence approximately accounting for many-body, size quantization, and finite temperature effects.

[38]R. Del Sole and R. Girlanda, Phys. Rev. B **48**, 11789 (1993).

[39]Y.-W. Mo, D. E. Savage, B. S. Swartzentruber, and M. G. Lagally, Phys. Rev. Lett. **65**, 1020 (1990).

[40]J. R. Power, P. Weightman, S. Bose, A. I. Shkrebtii, and R. Del Sole, Phys. Rev. Lett. **80**, 3133 (1998).

[41]S. Cereda and F. Montalenti, Phys. Rev. B **81**, 125439 (2010).

[42]N. Motta, A. Sgarlata, R. Calarco, Q. Nguyen, J. Castro Cal, F. Patella, A. Balzarotti, and M. De Crescenzi, Surf. Sci. **406**, 254 (1998).

[43]Other "diffuse"-like structures considered yielded relatively higher formation energies (by several meV/Å^2).

[44]Instead, beyond 4 ML, excess Ge tends to form clusters and the RAS simply attenuates as the proportion of the RS domain diminishes.

[45]T. Zhou, G. Renaud, C. Revenant, J. Issartel, T. U. Schülli, R. Felici, and A. Malachias, Phys. Rev. B **83**, 195426 (2011).